

Role of MRI Imaging Physics in Effect of TiO₂ on Hepatocellular carcinoma (Hep-G-2)

Hala Moustafa Ahmed¹, Mohamed Samieh NasrEldin², Ahmed Salah Abdelhady³, Abdelhady Abdelmohsen Abdelmonem⁴, Gehad Esam Mohamed⁵

Medical Biophysics-Biomedical Equipment Department¹-Radiology Department^{2,3,4and5}-Faculty of applied medical sciences October 6 University.

³Corresponding author: Ahmed Salah Abdelhady, Department of Radiology, Faculty of applied medical sciences, October 6 University, Egypt.

ABSTRACT:- Magnetic resonance imaging (MRI) has developed at an exponential rate over the last decades, and is now widely used as an anatomical and functional medical imaging modality. The applications of nanotechnology are nanoparticles which generate either “positive” or “negative” contrast in MRI. It addresses the main considerations guiding the synthesis and the characterization of TiO₂ nanoparticles based on the elements. In this study, the biosafety of TiO₂ NPs (7-10 nm) were evaluated after injection into the Hep-G-2. The results show that only a highly significant TiO₂ NPs element accumulation in the Hep-G-2. Our results showed that under a low dose (5 mg/kg), both NP types had no significant toxicity in cells. Janus NPs certainly seem less toxic than TiO₂ NPs in rats at 10, 15 mg/wells.

Keywords:Hep-G-2, Nanoparticles (NPs), MRI.

Introduction:-

Cancer is getting a huge problem day by day all over the world. Every day, many numbers of people are diagnosed with cancer disease. Despite of all the new drugs found, thousands of studies and methods developed, there is no exact and known treatment for cancer. One of the methods is nanotechnology and the usage of nanotechnology products or systems in cancer studies [1].

Developments in nanotechnology suggest new mechanisms to cure many human diseases, despite lack of knowledge about possible interactions between nanotechnology tools and biological tissues or cells. For example, gold nanoparticles for X-ray, magnetic nanoparticles for Magnetic Resonance Imaging (MRI) and other nanoparticles such as hybrid nanoparticles (iron oxide with gold) for both MRI and computed tomography (CT) are used as contrast agents [2, 3, and 4]. Cytotoxicity studies using Ni NPs were evaluated by means of mammalian models [5].TiO₂ is a white, odorless and non-combustible powder. There are many different names for titanium dioxide such as titanium (IV) oxide, titania, titanilic acid anhydride and Ti white. Titanium dioxide has two crystal structures; these are rutile and anatase which is more chemically active. Rutile form of titanium dioxide nanoparticles are also named as titanium dioxide fine particles (FP). As the anatase crystal structure increases, production of reactive oxygen species increases, too. Therefore, it is thought that the anatase titanium dioxide is more toxic to healthy cells than the rutile titanium dioxide. The rutile titanium dioxide is considered as chemically inert but when the particles become smaller, the surface area will increase and therefore the rutile titanium dioxide particles can become harmful according to the studies. Also the modifications that are done on the surface of nanoparticles cause changes in the activity of titanium dioxide particles [6].

Aim of the work:-

The main objective of this work is to find TiO₂ the control Hep-G-2 cell growth .We investigated the effects of TiO₂ on cell cycle regulation and magnetic resonance imaging..

Materials and methods:-

1-Cell lines and cell culture:

Cell lines and cell culture Cell monolayers of the human hepatoma cell line HepG-2 were purchased from VACSERA [Giza,Egypt]. HepG-2 cells were subculture in a 75 cm² flasks in DMEM supplemented with 2 mM L-glutamine [Biochrom], penicillin [Biochrom], streptomycin [Biochrom] and 10% heat inactivated fetal bovine serum [HyClone, UK] at 37°C under a humidified atmosphere containing 5.2% CO₂ saturated atmosphere until confluent monolayer detected and maintained in an exponential growth state [7]. Inoculated bottles were daily microscopically observed for 7 days for detection of cellular changes and development of cytopathic effect (CPE). Flasks developed CPE were freeze and thawed three times for virus extraction [8].

2- Synthesis of Nanoparticles:-

TiO₂ composite NPs were synthesized by the solvent-thermal method as stated in our previous work. First, TiO₂ NPs (about 7–10 nm) were synthesized based on a previously reported method [11]. Then, prepared TiO₂ NPs were centrifuged and washed with ethanol and redispersed in 10 mL *n*-hexane. Next, ferric acetylacetonate (17 mg) was dissolved in oleic acid (4 mL) and *n*-octyl alcohol (12 mL), and then added to a Teflon tube that had been autoclaved for 3 hours at 240°C. Then, the mixture was washed with ethanol and dispersed into a nonpolar solvent. TiO₂ NPs (1 mL dispersed in *n*-hexane) were dropped into the ferric acetylacetonate solution. The mixture was stirred for 4 hours before increasing the temperature to 70°C, in order to evaporate the *n*-hexane. Finally, the mixture was cooled to room temperature and transferred into a reaction kettle. The reaction temperature was kept at 240°C for 3 hours [9]. Finally, the prepared Fe₃O₄-TiO₂ NPs were centrifuged, washed with ethanol three times, and dispersed into 10 mL cyclohexane. Later, F127 triblock polymer was used to transfer the phase from organic to aqueous. Fe₃O₄-TiO₂ NPs (1 mL) were added dropwise to F127 (700 mg) and dispersed in CHCl₃ (70 mL). After the solution had been stirred for 4 hours, water (10 mL) was added and CHCl₃ evaporated using a rotatory evaporator. Finally, the aqueous dispersed NPs were washed with ethanol and redispersed in water [10].

3-Uptake assay:-

When the cells reached 70% confluence, the target cells were exposed to the vehicle, or 8 nM TiO₂ at 37°C. All assays were performed in triplicate. After 12, 24 and 36 hours of incubation, the free TiO₂ in the cell cultures were removed by washing the plated cells twice with the PBS buffer. The number of cells was counted with a hemocytometer. Two ml of 20% HNO₃ was added to each sample to lyse the cells. [11]

4-Magnetic Resonance Imaging (MRI):-

The phenomenon of NMR describes the absorption of electromagnetic energy by atomic nuclei in an external magnetic field. It relies on the quantum mechanical effect that many nuclei carry a spin and therefore a magnetic moment. When such a sample is exposed to a strong, homogeneous, polarizing magnetic field, a small magnetization along this field is induced inside the sample. The orientation of this magnetization can be manipulated by irradiating the sample with an isotope-specific resonance frequency, the so-called Larmor frequency, which is directly proportional to the strength of the polarizing field. The plates were positioned on the moveable examination table. The plate coil is a signal receiver that works with the MRI (1.5T) ESSENZA. Field strength (1.5 Tesla), Bore size (60 cm), System length (147 cm). Magnet technology Field strength (1.5 Tesla), Bore size (60 cm), Magnet length (131 cm), Helium consumption Zero Helium boil-off technology. Unit to create the images. The plates would be moved, feet first, into the magnet of the MRI unit and the technologist leaves the room while the MRI examination is performed. The total time spend on the MRI table would be between (30 and 60 minutes). [12-13] The scanning procedure was done using A Siemens (1.5T) MRI machine model, using head coil a different MRI sequences was performed (axial, coronal and sagittal) for scanning the phantom with different concentration (5mg, 10 mg, 15 mg) of TiO₂ NPs. The (t1) images were obtained using a conventional (axial sequence) with the following parameters: pulse repetition time (TR) = 776 ; echo time (TE) = 9.9 ; matrix size

=156*256s; field of view (FOV) 195*240 ; and slice thickness (ST) = 1.7 Mm,,The (t2) images were obtained using a conventional (sagittal sequence) with the following parameters: pulse repetition time (TR) 5890 ; echo time (TE) =86 ; matrix size =390*640; field of view (FOV) = 219*270.; and slice thickness (ST) = 1.7. m,,The (T2_tse3d_tra_p2) images were obtained using a conventional (axial sequence) with the following parameters: pulse repetition time (TR) = 550; echo time (TE) =109 ; matrix size =200*200; field of view (FOV) 512*512; and slice thickness (ST) = 1.7 m ,,The (T2 3d) images were obtained using a conventional (cor MRP Range(3)>) with the following parameters: pulse repetition time (TR) 550 ; echo time (TE) =109 ; matrix size =200*200; field of view (FOV) = 256*256.; and slice thickness (ST) = 1.7 m



Figure(1) phantom position on mri machine





5-Statistical Analysis:-

Continuous variables were recorded as mean \pm SD; ANOVA-f test, followed by Tukey's test, was used to evaluate the significance of difference ($P < 0.05$) among group. Data analysis was made by Fisher's exact and Pearson's correlation tests. Data were expressed as mean \pm standard error (S.E). Using SPSS for Widows (Chicago, IL, USA) when appropriate $p < 0.05$ was considered statistically significant. Histogram analysis combines techniques that compute statistics and measurements based on the gray-level intensities of the image pixel. The Student's t-test and other statistical analysis were performed using statistical SPSS -12 programs.

Results and discussions:-

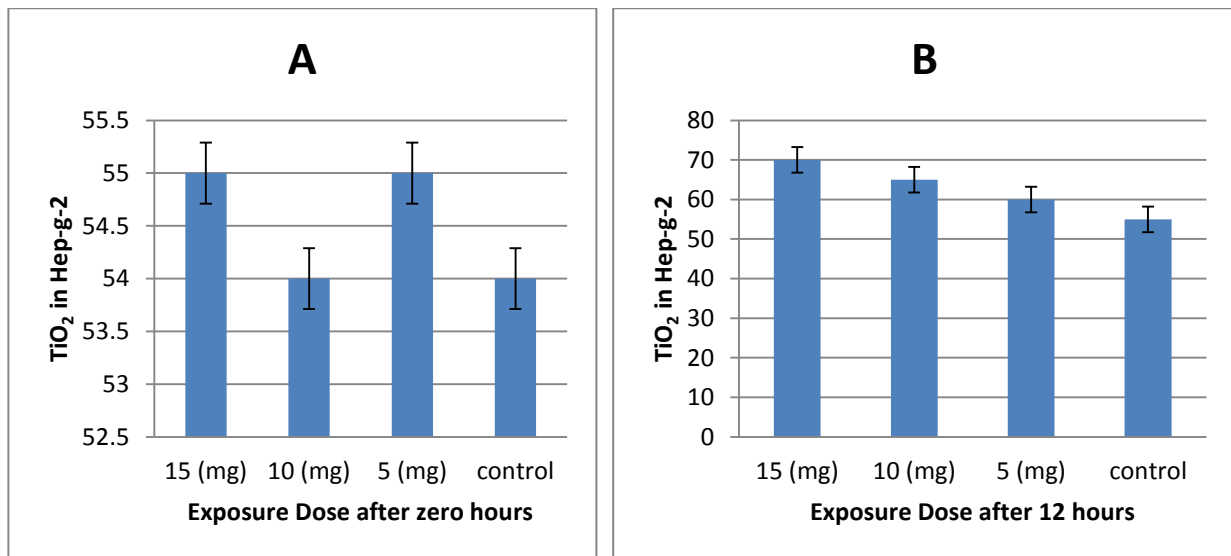
1- Effect of (TiO)₂ on Hepatocellular Carcinoma (Hep-G-2):-

Figure (2) where the cytological changes (70% CPE) could be detected within 48 hours post viral inoculation. The delayed detection of cytological changes may be attributed to the low viral load in collected specimens, recording 70% CPE on the 48 hours post infection. Alternating passaging in cell culture could be a supporting factor to maximize the viral load, where on the 5th passage the cytological changes could be detected within 2-4 days post viral infection showed a gradual increase in the mean viral infectivity titer relatively to time. (Figures 1) demonstrate that NPs induced 376.8 %, 14.9 % and 7.3 % inhibition rates in the Hep-G-2 cell viabilities, respectively. Following 2 hours incubation with GNPs, the cell viability of Hep-G-2 cells was further decreased, with an inhibition rate.

			
Figure (2-a): Control cell lines Cellular morphology Viral cells growth (minimal).	Figure (2-b): Cells were confluent and remained long and slender shape. Viral Activation of Hep-G2 (minimal) .Harping viral infection.at 12 hours	Figure (2-c): Celle all appeared long and spindle shaped.no sings. Cells could clearly at 24 hours	Figure (2-d): Celle all appeared long and spindle shaped. Minimal growth at 48 hours.

2- Distribution and uptake of TiO₂ on Hep-G-2 cells:-

TiO₂ levels in Hep-G-2 were used for evaluating the presence or distribution of TiO₂ composed in TiO₂ NPs in the cell culture. TiO₂ content in different concentrations on Hep-G-2 types is shown in figure 2 after exposed to with TiO₂ NPs, although statistical significance was found, which might have been due to individual differences. Hep-G-2 content in TiO₂ NP-treated at 5, 10 and 15 mg/wells showed a significant elevation ($P < 0.05$). No significant difference was found in TiO₂ content in 10 and 15 mg/wells TiO₂ NP-treated groups. Treatments of TiO₂ NPs resulted in only a slight change in 5 mg/wells content in the Hep-G-2 ($P > 0.05$). This results agree with a were at 24 h significantly reduced by 84.5% with GNPs plus Hep-G-2 cells. Combined 0.0025 ml GNPs plus Hep-G-2 cells resulted in a 97.7% inhibition of cyclin A protein at 24 h.[14]



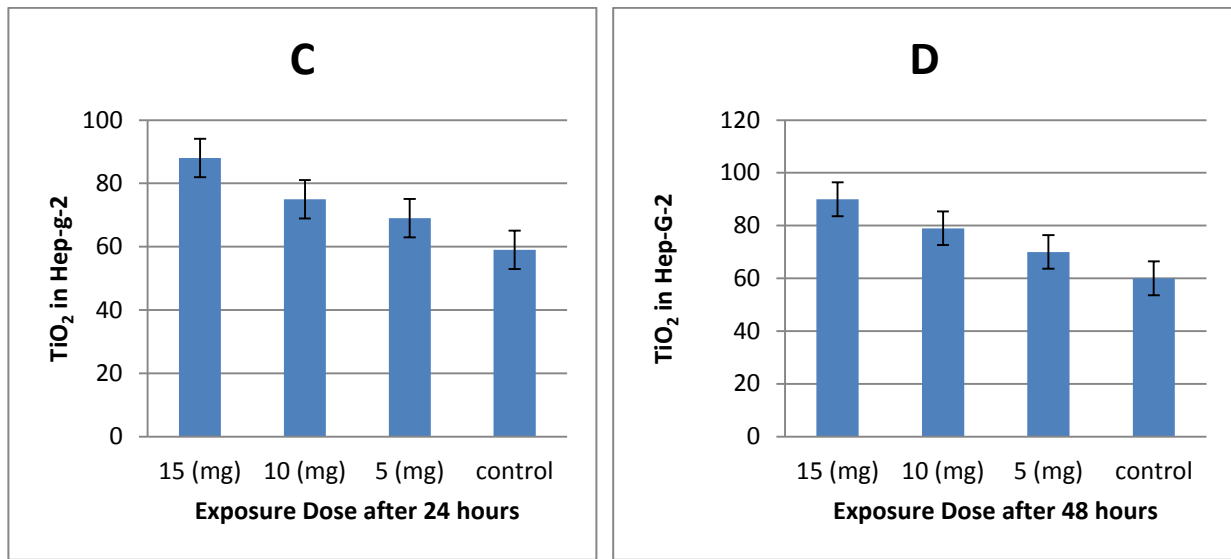


Figure 3: Nanoparticle (TiO₂) distribution and uptake on Hep-G-2 cells at (zero,12,24 and 48 hours)

3-Magnetic Resonance Imaging of the TiO₂ on Hep-G-2 cells:-

Table (1) :Indicate a significantly increased in (15 mg) as compared to (10 mg) (p<0.05).On the other hand, the Standard deviation (S.D) are presented in tables 1 , the (15mg) and (10mg) standard deviation levels of (22.62±8.15,23.09±8.91 mean, S.D) respectively. These indicate a significantly increased in (15mg) as compared to (10mg) (p<0.05). These indicate a significantly increased in (15mg) as compared to (10mg) (p<0.001).Thus, the statistical analysis revealed that COV of (0.54 ± 0.20. 0.8 ± 0.08 mean, S.D) respectively. These indicate a significantly increased in (15mg) compared to (10mg) (p<0.001) [15.16].

Items	Concentration 15 mg	Concentration 10 mg	P
Mean			
Min. - Max.	26.55 - 114.70	120.99 - 258.99	<0.001*
Mean ± S.D	74.12 ± 24.80	218.45 ± 25.52	
Median	76.44	226.91	
S.D			
Min. - Max.	6.31 - 39.18	8.44 - 47.95	0.001*
Mean ± S.D	22.62 ± 8.12	23.09 ± 8.91	
Median	10.37	22.04	
Median			
Min. - Max.	11.0 - 114.0	120.0 - 252.0	<0.001*
Mean ± S.D	72.43 ± 27.31	221.90 ± 26.38	
Median	75.50	228.50	
COV			
Min. - Max.	0.08 - 0.89	0.05 - 0.28	0.003*
Mean ± S.D	0.54 ± 0.20	0.8 ± 0.08	
Median	0.13	0.10	

Table (1): Comparison between the two studied group's concentrations 15 mg and 10 mg according to Mean, Standard Deviation, Median and Coefficient of Variation of different parameters using MRI.

p: p value for Student t-test.*Significant at level < 0.05 .** Highly Significant level < 0.0001 .*** Not significant level > 0.05 . Note: ** $P < 0.01$, *** $P < 0.001$ compared with control.

Conclusion:-

The present study demonstrated that the enhancement of nano particles TiO_2 that deteriorates hepatocellular carcinomaHep-G-2 growth will be promising method for the treatment of growth hepatocellular carcinomaHep-G-2.

Conflict of Interest:-

The authors declare no competing interests regarding the publication of this paper.

Acknowledgements:-

The authors would like to thank dr/eman zaglol , dr/ Mohamed hamam , dr/Diana Abaas and Dr/Hussein abid.

References:-

- [1] Bogdan J, Pławińska-Czarnak J, Zarzyńska J. Nanoparticles of Titanium and Zinc Oxides as Novel Agents in Tumor Treatment: a Review. *Nanoscale Res. Lett.* [Internet]. 2017;12:225. Available from: <http://nanoscalereslett.springeropen.com/articles/10.1186/s11671-017-2007-y>.
- [2] Hainfeld JF, Slatkin DN, Focella TM, et al. Gold nanoparticles: a new X-ray contrast agent. *Br. J. Radiol.* [Internet]. 2006; 79:248–253. Available from: <http://www.ncbi.nlm.nih.gov/pubmed/16498039>.
- [3] Fang C, Zhang M. Multifunctional magnetic nanoparticles for medical imaging applications. *J. Mater. Chem.* 2009;19:6258–6266.
- [4] Kim D, Yu MK, Lee TS, et al. Amphiphilic polymer-coated hybrid nanoparticles as CT/MRI dual contrast agents. *Nanotechnology* [Internet]. 2011;22:155101. Available from: <http://stacks.iop.org/0957-4484/22/i=15/a=155101?key=crossref.7dcab9aa9fc9fc14e08cf880e4c12dca>
- [5] M.Ahamed, H.A.Alhadlaq, Nickel nanoparticle-induced dose-dependent cytogenotoxicity in human breast carcinoma MCF-7 cells, *Onco.Targets Ther.* 7(2014) 269–280.
- [6] Magaye R, Shi H, Magaye R, et al. Titanium dioxide nanoparticles: A review of current toxicological data. *Fibre Toxicol.* 2013;10:1–33.
- [7] Paino IM, Marangoni VS, de Oliveira Rde C, Antunes LM, Zucolotto V. (2010) :Cytotoxicity and genotoxicity of gold nanoparticles in human hepatocellular carcinoma and peripheral blood mononuclear cells. *Toxicol Lett.*, 215: 119-125.
- [8] Bussereau F.; Benejean J. and Saghi N. Isolation and study of temperature-sensitive mutants of rabies virus. *Gen Virol.*, 1982; 60(pt1): 153-8.
- [9] Zeng L, Ren W, Xiang L, Zheng J, Chen B, Wu A. Multifunctional Fe_3O_4 - TiO_2 nanocomposites for magnetic resonance imaging and potential photodynamic therapy. *Nanoscale.* 2013;5(5):2107–2113.
- [10] Dinh CT, Nguyen TD, Kleitz F, Do TO. Shape-controlled synthesis of highly crystalline titania nanocrystals. *ACS Nano.* 2009;3(11):3737–3743.

- [11]Kong T et al 2008 Enhancement of radiation cytotoxicity in breast-cancer cells by localized attachment of gold nanoparticles *Small* 4 1537–43.
- [12]Jacobs MA, Barker PB, Bluemke DA, et al. Benign and malignant breast lesions: diagnosis with multiparametric MR imaging. *Radiology*. 2003; 229:225- 232.
- [13]Shahar KH, Solaiyappan M, Bluemke DA. Quantitative differentiation of breast lesions based on threedimensional morphology from magnetic resonance imaging. *J Comput Assist Tomogr*. 2002; 26:1047-1053.
- [14]Iliakis G and Nusse M 1983 Evidence that repair and expression of potentially lethal damage cause the variations in cell survival after x irradiation observed through the cell cycle in Ehrlich ascites tumor cells *Radiat. Res.* 95 87–107
- [15].Ke, S.; Zhou, T.; Yang, P.; Wang, Y.; Zhang, P.; Chen, K.; Ren, L.; Ye, S. :Gold nanoparticles enhance TRAIL sensitivity through Drpl-mediated apoptotic and autophagic mitochondrial fission in NSCLC cells. *Int. J. Nanomed.* 2017, 12, 2531–2551.
- [16]Hainan Sun 1, Jianbo Jia 1,2 ID , Cuijuan Jiang 3 and Shumei Zhai 1 :Gold Nanoparticle-Induced Cell Death and Potential Applications in Nanomedicine *Int. J. Mol. Sci.* 2018, 19, 754; doi:10.3390/ijms19030754